2010-36-0547

The Application of the Singular Value Decomposition (SVD) for the Decoupling of the Vibratory Reproduction System of an Aircraft Cabin Simulator

Luiz Chamon, Giuliano Quiqueto and Sylvio Bistafa
Noise & Vibration Group – Polytechnic School of the University of São Paulo

ABSTRACT

Mechanical systems excited by vibratory point-sources, tend to suffer from interference among axes, due to characteristics of the reproduction system or difficulties associated with the application of the excitation forces on the system's mass-center. Thus, when it is necessary to excite the system independently in different directions, control techniques are needed for the correct reproduction of the desired signals. This work presents the developments for the reproduction of vibrations in two directions, on platforms employed as the base of seats of an aircraft cabin simulator. Each platform is independently excited by two orthogonal shakers, located in the geometrical center of the latter. Based on an evaluation of the degree of coupling between both orthogonal axes, signal processing solutions for the decoupling problem are proposed. Using SVD to diagonalize the transfer-function-matrix, an independent base for the system was identified. Some preliminary evaluations using inverse static filters show that the proposed method can provide the desired results.

INTRODUCTION

Nowadays, the airplane is one of the most important means of transportation. Beyond its known speed, these airborne vehicles are safe and extremely efficient, due to their collective nature. All the aforementioned, along with the ever sinking prices, lead to an increase in the number of passengers and miles flown [1]. With that in mind, the aeronautic industry has recently started to give more attention to the comfort of passengers, trying to meet the continuous demand for more silent and smoother flights.

The vibratory environment in an aircraft cabin is mainly composed of two elements: oscillatory motion generated from rotating parts and the motion caused by the passage through non-uniform airflow. The first component appears in the form of narrow band excitations, while the second, dominant in fixed-wing aircrafts, generates a sort of uniform random vibration with one or two peaks from 0.5 to 5 Hz. As long as there is no heavy turbulence, the experienced accelerations are not notably stronger than those found when travelling by car (Figure 1) [2].

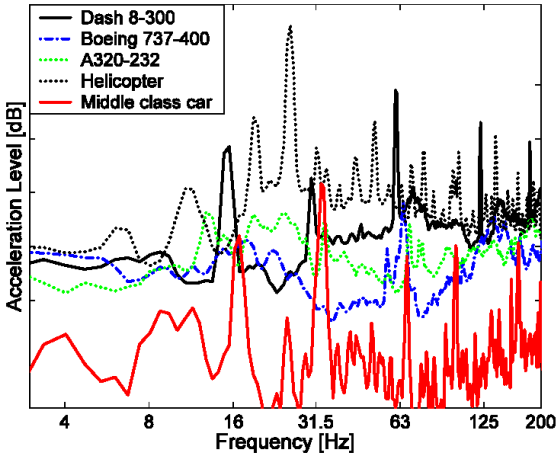

Figure 1: z-axis vibration levels for different transport types [3]

Inside the cabin, most of the excitation is concentrated between the y- (side horizontal) and z-axes (vertical). Since in the direction of flight (x) the level is from 5 to 10 dB lower and due to the reduced sensitivity of the human body to horizontal vibrations, it has been neglected throughout this text [3,4].

The article is organized as follows. After this introduction, the vibration reproduction system of the cabin simulator is presented, followed by a simple modeling of its process. The theory of singular value decomposition is then presented and its use in the solution of the problem is studied. A system simulation involving field acquired data and a sensitivity analysis conclude this paper.

VIBRATION REPRODUCTION

In order to study the comfort of passengers, an aircraft cabin simulator is being developed at the University of São Paulo, in a joint effort between several universities and the aeronautical industry. Based on a general commercial aircraft, it comprises air conditioning, pressurization and vibroacoustic reproduction systems, in order to provide users with a full airplane experience (Figure 2).

The subsystem in charge of the reproduction of vibration signals is composed of two collocated perpendicular shakers mounted underneath the uncoupled floor pieces that support every pair of seats (Figure 3). Each actuator is responsible for exciting one of the axes defined earlier without interfering considerably with the other. Though it might seem straightforward, unbalanced mass distributions and application of forces away from the exact mass-center generates serious coupling, making it almost impossible to reproduce perfectly the desired vibration field.

Furthermore, the shakers response has to be taken into account, as well as the shakers coupling to the floor and the path of transmission to the rail next to the seat, where the reference measurements are taken.

Figure 2: Interior of the cabin simulator

Figure 3: Vibration reproduction system

SYSTEM MODELING

The block diagram of the Dual-Input Dual-Output (DIDO) system for the two-axis vibration exciter is shown in Figure 4, where y and z denote the input and ψ and ζ the output signals for the y- and z-axes, respectively. From this notation, it arises naturally that the transfer functions (TF) $H_{y\psi}$ and $H_{z\zeta}$ describe the actuators (direct path) and that $H_{y\zeta}$ and $H_{z\psi}$ are the coupling elements (cross path).

This model assumes that the system is perfectly linear, which is a fairly reasonable hypothesis for the excitation levels the structure will be submitted to. Furthermore, small nonlinearities can be seen as output noise without invalidating the analysis, though efforts shall be made to treat them separately.

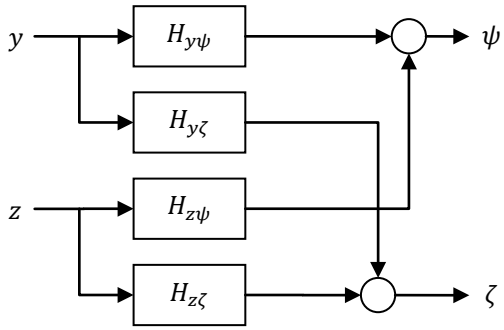

Figure 4: Block diagram of the reproduction system

The above diagram can be described in the matrix form (Eq. 1), which gives rise to the idea of diagonalization as a mean to decouple the system [5].

$$\boldsymbol{O} = \boldsymbol{HI} \Leftrightarrow \begin{bmatrix} \psi \\ \zeta \end{bmatrix} = \begin{bmatrix} H_{y\psi} & H_{z\psi} \\ H_{y\zeta} & H_{z\zeta} \end{bmatrix} \begin{bmatrix} y \\ z \end{bmatrix} \quad (1)$$

DIAGONAL DOMINANCE

In order to evaluate the coupling element's influence, it is usual to analyze the diagonal behavior of the multivariate system. The importance of off-diagonal elements in the matrix $\boldsymbol{H}$, i.e. the cross-axes interaction, can be defined as [6]

$$\boldsymbol{E} = \left(\boldsymbol{H} - \widetilde{\boldsymbol{H}}\right)\widetilde{\boldsymbol{H}}^{-1} \quad (2)$$

where $\widetilde{\boldsymbol{H}}$ is the matrix composed only by the diagonal elements of $\boldsymbol{H}$.

It can be shown that, if $\boldsymbol{E}$ is small, than the elements outside the diagonal have little influence on the system and it is almost uncoupled. The transfer function matrix is then said to be diagonal dominant. Furthermore, diagonal dominance can be shown to relate with the Gershgorin radius ϱ_i, defined as [5]:

$$\varrho_i(f) = \frac{\sum_{j \neq i} |H_{ij}(f)|}{|H_{ii}(f)|} \quad (3)$$

where $|H_{ij}(f)|$ denotes the magnitude of the TF from i to j at frequency f.

The smaller the Gershgorin radii, the more diagonal dominant the matrix will be and the less coupled the system, meaning ultimately the interactions between axes will be small. As a rule of thumb, a plant can be said diagonal dominant at all frequencies where $\varrho_i \leq 0.5$ [5].

Though this criterion is usually applied as a stability condition for closed-loop control systems, it has a deeper meaning when applied to matrices in general. The Gershgorin theorem states that any complex matrix has its eigenvalues in the union of the circles centered on the diagonal elements and with radius equal to the sum of the absolute value of the other row elements ($\sum_{j \neq i} |a_{ij}|$). It becomes then clear that the fraction previously defined becomes small as the matrix approaches a diagonal one.

SVD

Singular values decomposition is a matrix factorization method which emerges from the eigenvalue decomposition (EVD) of symmetric matrices: $\boldsymbol{A} = \boldsymbol{Q}\boldsymbol{\Lambda}\boldsymbol{Q}^H$, where $\boldsymbol{Q}$ is the unitary eigenvector matrix, $\boldsymbol{\Lambda}$ is the eigenvalues diagonal matrix and $(\cdot)^H$ denotes the conjugate transpose. Though Hermitian or symmetric real matrices always have such decomposition, this is not necessarily true in general. On the other hand, if it is allowed for matrices on both sides to be any unitary matrix (not necessarily the same), the factorization becomes possible again.

At this point, SVD can be defined as

$$\boldsymbol{A} = \boldsymbol{U}\boldsymbol{\Sigma}\boldsymbol{V}^H, \quad (4)$$

where $\boldsymbol{A}$ is any m by n matrix; $\boldsymbol{U}$ (m by m) and $\boldsymbol{V}$ (n by n) are two unitary matrices, so that the columns of $\boldsymbol{U}$ are eigenvectors of $\boldsymbol{A}\boldsymbol{A}^H$ and those of $\boldsymbol{V}$ are eigenvectors of $\boldsymbol{A}^H\boldsymbol{A}$; and finally $\boldsymbol{\Sigma}$ (m by n) has on its diagonal the so called singular values of $\boldsymbol{A}$ (σ_i), which are the square root of the nonzero eigenvalues of both $\boldsymbol{A}\boldsymbol{A}^H$ and $\boldsymbol{A}^H\boldsymbol{A}$ [7].

Even though it has higher computational cost than EVD, singular value decomposition has the great advantage of existing for any matrix. This allows it to be applied to any problem without worrying whether it is defective or not, i.e. if it is diagonalizable by EVD. Moreover, it provides a numerically robust way to invert matrices even when they are almost singular, computing an approximation called a *pseudoinverse*.

Given that both $\boldsymbol{U}$ and $\boldsymbol{V}$ are unitary, the inverse of $\boldsymbol{A}$ (when it exists) can be written as

$$\boldsymbol{A}^{-1} = \boldsymbol{V}diag\{1/\sigma_i\}\boldsymbol{U}^H, \quad (5)$$

where $diag\{n_i\}$ is the diagonal matrix whose elements are n_i.

The pseudoinverse, sometimes noted $\boldsymbol{A}^+$, is calculated in much the same way, the only difference being that all small σ_i are replaced by 0 instead of inverted. Upon doing such, directions that were before highly corrupted by round off errors are left out, allowing for a much more robust solution to the inversion problem [8].

DECOUPLING EQUALIZERS

Equation 6 shows the result of applying the factorization above to the problem set in Eq. 1. It can be seen that the isometries $\boldsymbol{U}$ and $\boldsymbol{V}^H$ build a base where the system is uncoupled, making it possible to design independent Single-Input Single-Output (SISO) equalizers. The value of σ represent, then, the gain applied by the system at each frequency band.

$$\begin{bmatrix} \psi \\ \zeta \end{bmatrix} = \underbrace{\begin{bmatrix} U_{m\psi} & U_{n\psi} \\ U_{m\zeta} & U_{n\zeta} \end{bmatrix} \begin{bmatrix} \sigma_m & 0 \\ 0 & \sigma_n \end{bmatrix} \begin{bmatrix} V_{my} & V_{ny} \\ V_{mz} & V_{nz} \end{bmatrix}^H}_{\boldsymbol{H}} \begin{bmatrix} y \\ z \end{bmatrix} \quad (6)$$

Using the concepts discussed above, two SISO systems can be added to compensate the system's behavior. This way,

$$\tilde{\boldsymbol{I}} = \boldsymbol{H}\boldsymbol{H}^+\boldsymbol{I} = \boldsymbol{H}(\boldsymbol{V}\boldsymbol{G}\boldsymbol{U}^H)\boldsymbol{I}, \quad (7)$$

where $\boldsymbol{G}$ denotes the diagonal matrix of independent quasi-ideal SISO equalizers. Note should be taken that we exempt ourselves from perfectly inverting the system's transfer function matrix, using the concept of pseudoinverse instead. It has the advantage of avoiding spending a lot of energy in what could very well be a node of the structure. Since these modes are very hard to control to say the least, it is a worthless effort trying to compensate them. What is intended here as "very hard to control" depends both on the application and the designer's discretion. Figure 5 illustrates an implementation of the above equation.

Although this solution seems appealing, it has serious drawbacks that have to be taken under review. Firstly, as decoupling is achieved through the coordination of actuators, the failure of one of them may affect the behavior of the whole system. On a second matter, this method is very sensitive to modeling errors or noise, especially for ill-conditioned matrices [5]. Last but not least, singular value decomposition is unique for every matrix (except for columns swap) which makes it hard to use adaptively, since every change in the system demands a new factorization [7].

Notwithstanding all of the above, the fact that the SVD algorithm is iteratively convergent can actually be useful in practice [8]. Since it is only necessary for the TF matrix to be diagonal dominant in order for any loop to be stable [5], or for the system to be approximately inverted, few iterations might suffice for small matrices. If the input signals are sufficiently uncorrelated, techniques from [9] can be used to determine an approximate TF matrix and SVD could then be applied to dynamically decouple any given system.

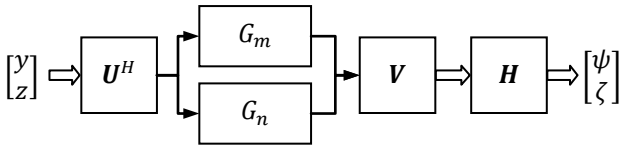

Figure 5: Block diagram of the uncoupling equalizer

RESULTS

Measurement procedures

To assess the elements in the model, the linearity property of the system was used. The y-related TFs were evaluated leaving the z-axis unexcited and vice-versa. This allows having a clear view on each part's contribution to the direct and cross-path.

In order to get a more realistic representation of the environment under which the reproduction will occur, the testing signal were chosen as white noise, which has several advantages over sine testing. Though the latter require less power, it puts a lot of energy at a single frequency, which doesn't account for multiple resonance effects. Moreover, the sine sweep rate has to be made extremely slow, so as to assure the proper excitation of all important modes [10]. This could considerably increase the testing time, which was set to 5 minutes in order to guarantee good spectral resolution and averaging [9].

Spectral analysis

The transmission paths frequency responses can be found, along with their coherence functions, in Figure 7 and 8.

As can be seen, the y-axis related coherences are much lower than those of z, probably due to the bad coupling provided by the support system (Figure 3). Overall, the reproduction due to vertical excitation tends to be more accurate and flat, even in cross-axis. Moreover, all TFs can be seen to have a low cutoff frequency around 20 Hz, below which they fall considerably, probably owed to the reduced size of the floor and the control sensor being positioned close to a support point. The notches found in the coherence function at harmonics of 60 Hz can be attributed to power supply interference at the input. Following, each transfer function shall now be summarily analyzed as described in [9].

$H_{y\psi}$ is one of the direct transmission paths. It has fairly low coherence, which makes the average normalized error of its estimation scale up to one of the highest among the evaluated TFs (around 0.28). The drop in both the frequency response and the coherence function around 170 and above 200 Hz suggests the presence of extraneous noise at the output (measurement point). A sharp fall around 13 Hz can be attributed to some nonlinear behavior of the system, probably a mechanical resonance of the structure.

The other direct excitation element, namely $H_{z\zeta}$, describes a much better coupled actuator, i.e. it has high coherence and close to 0 dB magnitude. Even so, broad falls around 40 and 125 Hz again suggest noise disturbance at the control sensor. In opposition to above, two notches in low frequencies are of very different nature: the one around 19 Hz is due solely to spectral resolution error, while the one at 29 Hz is a nonlinearity of the plant. This can be assessed noting that the latter will remains invariant to changes in the spectral resolution.

The y-direction is coupled with ζ through the $H_{y\zeta}$ block. It has most the same characteristics of the direct y-axis reproduction, with serious extraneous perturbations at the output between 100 and 150 Hz, around 170 Hz, and above 200 Hz. Furthermore, nonlinearities appear around 12 and 27 Hz. This particular cross-axis reproduction is specially intricate since it involves complicated processes, e.g. rotational modes. Its highly disturbed behavior beyond 100 Hz testifies to that.

At last, $H_{z\psi}$ represents the cross-axis influence of direction z on ψ, which can be seen to couple even better to the latter than the y reproduction axis did. This can be related directly to the construction of the actuator's support. Furthermore, both coherence function and frequency response magnitude drop broadly around 150 and 240 Hz, indicating issues with noise in the measurements. On the count of nonlinear response, notches around 15 and 30 Hz suggest, again, possible resonances around these bands.

The error presented in Figure 9 is the difference between a real vibration signal passed through the actual reproduction system and through the modeled one. The mean error is 3.56 dB for the ψ-axis and 3.81 dB for the ζ-axis. Though this figure is reasonable in the sphere of human sensation, the high standard deviations show a lack of stability throughout the spectrum, due mainly to great error in the low frequency region. As noted previously, measurement noise and nonlinearities in that range are responsible for the unfitness of the model. Different techniques or even sensor positions should be studied in order to achieve more robust system identification.

Diagonal dominance

In order to justify the decoupling of the system, the aforementioned Gershgorin radius was evaluated for each frequency (Figure 6). The green line represents the threshold

defined earlier, above which the system cannot be considered diagonal dominant anymore.

The good coupling between z and ζ is responsible for the fairly diagonal behavior of the latter axis at most frequencies.

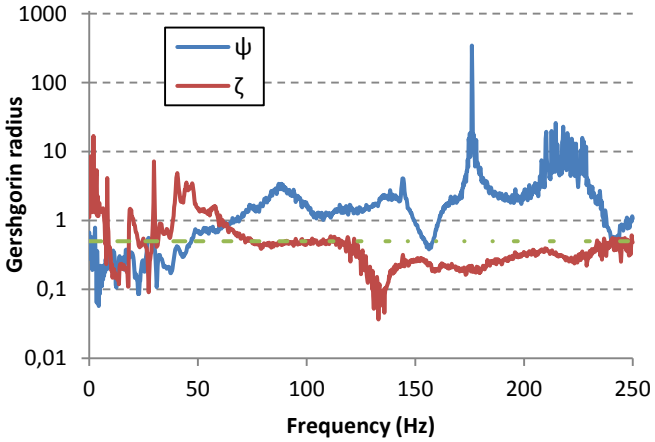

Figure 6: Gershgorin radius of the coupled system

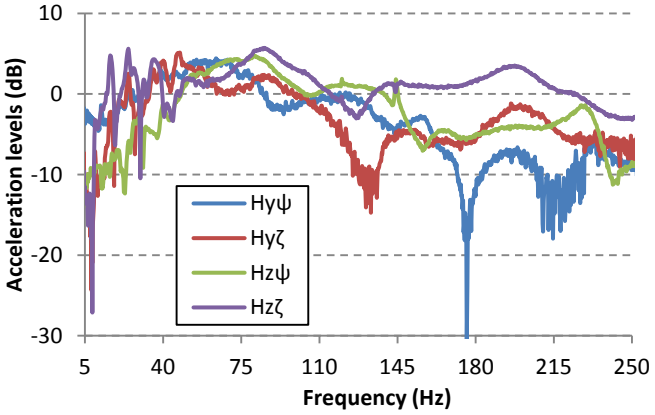

Figure 7: Frequency response of the transmission paths

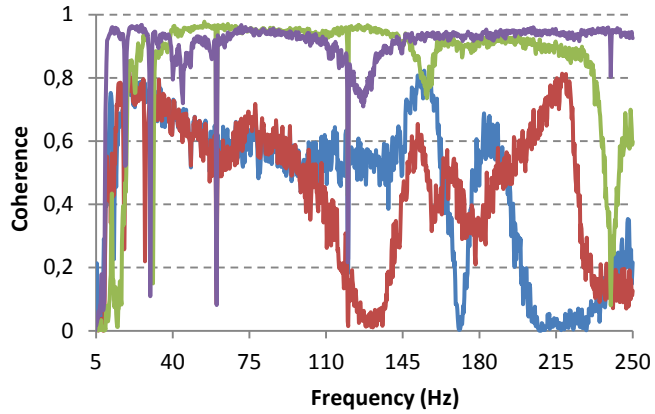

Figure 8: Coherence functions (same legend as above)

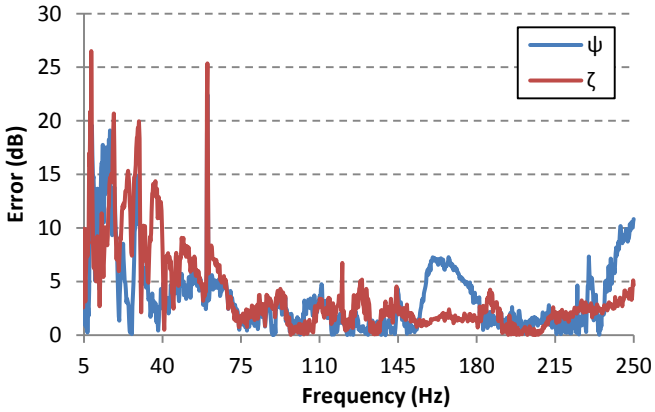

Figure 9: Error in the linear modeling of the reproduction system

Decoupling equalizer design and simulation

In order to design the decoupling equalizers, a variation of the pseudoinverse technique was devised. Given that $\boldsymbol{U}$ and $\boldsymbol{V}$ are isometries, the gain of the filters will be determined exclusively by the singular values. Using this fact, instead of zeroing the inverse of small σ_i, a saturation function was applied. This transformation allows preserving the overall shape of the function, causing small divergence in possibly already causal frequency responses. Moreover, this process makes errors caused by mismatching between pseudo and actual inverse to come in the form of narrow peaks, which are more likely to average out and become imperceptible. For the purpose of this work, the maximum gain of the inverse filters was set to 20 dB applying a hyperbolic tangent function on all singular values under 0.033 (inverse gain above 15 dB).

A frequency-domain simulation of the system using the previously assessed model returned the results showed in Figure 10. It shows the mismatch as defined in Eq. 8, which represents the gain deviation from a perfectly inversed TF. $\boldsymbol{H}(f)$ denotes the transfer function matrix and $m(f)$, the scalar mismatch at frequency f.

As predicted, the pseudoinverse technique proposed previously behaved extremely well under the conditions of the simulation. Even so, it should be noted that the frequency regions where the errors occurred were mentioned before as unreliable due to noisy measurements. This susceptibility to noise and errors in the determination of the frequency response of the TF matrix is a well known issue of static decoupling [6] and the main reason why it is not recommended for applications in which the system's structure changes over time.

$$\begin{bmatrix} m_\psi(f) \\ m_\zeta(f) \end{bmatrix} = H(f)H^+(f)\begin{bmatrix} 1 \\ 1 \end{bmatrix} \quad \textbf{(8)}$$

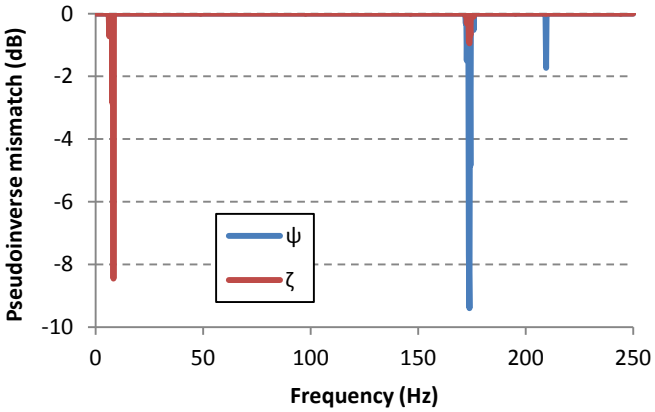

Figure 10: Decoupling equalizers mismatch (deviation from perfect inverse)

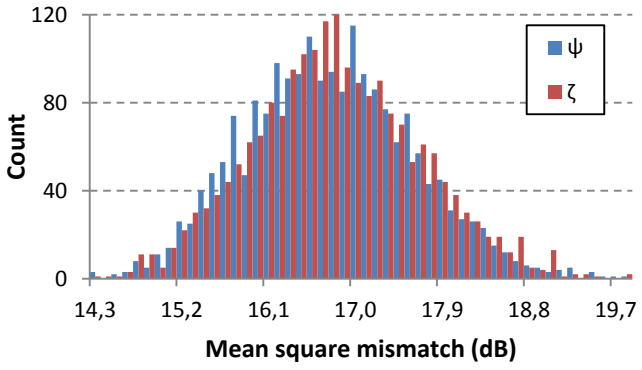

Figure 11: Decoupling equalizers mismatch due to Gaussian random error in the model

Monte Carlo sensitivity analysis

As a mean to evaluate the sensitivity of the static decoupling equalizers to changes or errors in the TF matrix, a Monte Carlo type investigation is now presented. A zero-mean Gaussian complex disturbance was added to all four elements of the model over the whole spectrum.

To have a global idea of the mismatch behavior its ℓ^2-norm was calculated as

$$e = \left(\sum_f m(f)^2 \right)^{1/2} \quad (9)$$

This metric is inspired on the fact that most research on human response to vibration rely on the RMS of the excitation signal, though it has been argued that a 4th power based value describes more accurately the human sensation [4].

An example of the results of such study is presented in the histogram of Figure 11, for an error magnitude variance of 0.01, which is roughly equivalent to a variation from 1 to 3 dB, depending on the element's original gain. It is important to note that for the undisturbed system $e_\psi = 4.26$ dB and $e_\zeta = 2.87$ dB.

Already at this point, it is clear that errors in the estimation of the TFs or changes in the system's behavior reflect highly on the quality of the feedforward decoupling equalizer's performance. While the mean initial error was set around 3 dB, which is slightly above the human differential threshold defined in [4], it has grown up to 16 dB, becoming clearly noticeable.

The aforementioned experiment was repeated for different error variances. The means, standard deviations, maximum and minimum values of the mean square mismatch are showed in Figure 12 and 13. The average change introduced by the perturbation on the magnitude of the TFs goes up to 2 dB.

The mismatch grows rapidly with the errors, as the SVD-based pseudoinverse loses effectiveness. As mentioned before, modeling errors and changes in dynamic behavior are performance limiters of static feedforward filters, and the results provided in this section come to corroborate these statements.

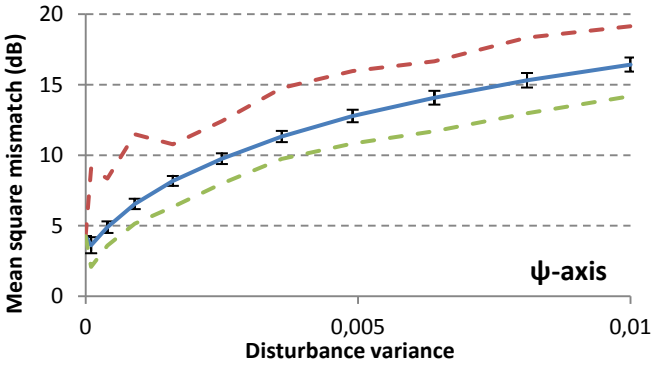

Figure 12: Mean square mismatch on the ψ-axis for different disturbance variances

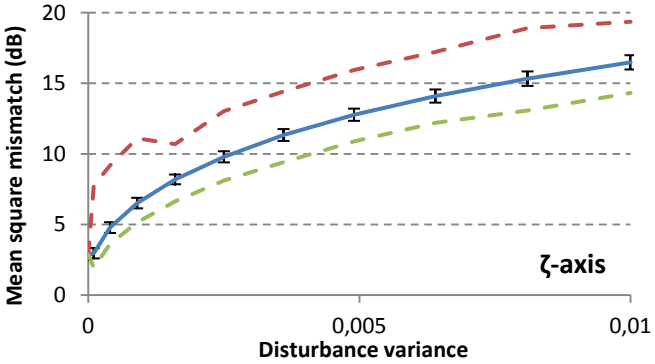

Figure 13: Mean square mismatch on the ζ-axis for different disturbance variances

So far, only the inversion performance has been studied, leaving aside the decoupling robustness. To evaluate this characteristic, we calculated the frequency-averaged

Gershgorin radius. The maximum value is also shown in Figure 14 and 15.

The ψ row is less sensitive than the ζ one, since its contribution to both axes is far smaller, as seen through its low coherence function. At any disturbance rate, ϱ_{ψ} is smaller than 0.5 and, thus, does not influence the diagonal dominance of the system.

On the other hand, ϱ_{ζ} behaves much worst. Though its mean value stays under the upper limit, the maximum radius rapidly grows above it. This difference shows that at some frequencies the system is harder to uncouple than others.

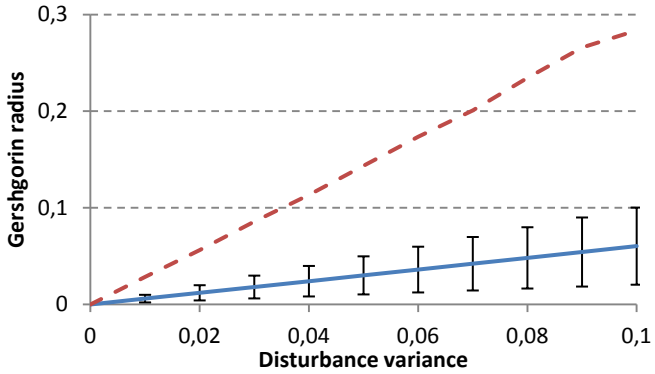

Figure 14: ψ row mean and maximum Gershgorin radius for different disturbance variances

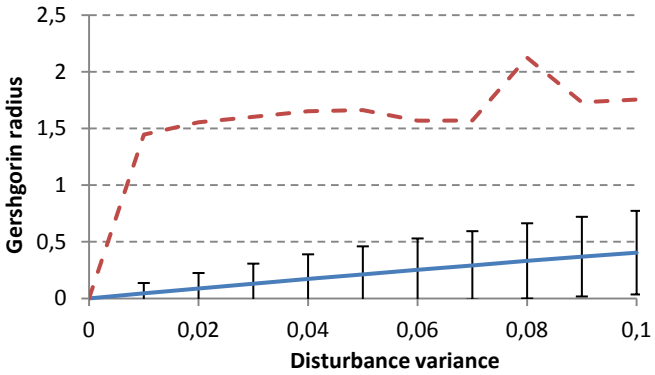

Figure 15: ζ row mean and maximum Gershgorin radius for different disturbance variances

CONCLUSION

The reproduction of multiaxial vibration using point-sources is a particularly complicated problem, due to the mechanical interaction between the axes. The SVD-based pseudoinverse method proposed proved to be efficient in both decoupling and compensating the system's frequency response. These preliminary results showed that, though the robustness of the static filters are low, the decoupling performance is sustained even in the presence of disturbance, so that further investigation on adaptive compensation of singular values could lead to improvements on the overall performance of the equalizers. The difference between the axes reproduction quality, which in this case reduces to coupling to the structure, determines the sensibility of the system to errors in that direction, making it less robust to changes on the related transfer functions.

REFERENCES

[1] United States of America. Bureau of Transportation Statistics, "National Transport Statistics", http://www.bts.gov/publications/national_transportation_statistics, 1 de ago. 2010.

[2] Quehl, J., "Comfort studies on aircraft interior sound and vibration", Ph.D thesis, Philosophy, Psychology and Sport Sciences Department, Carl von Ossietzky Universität, Oldenburg, 2001.

[3] Bellmann, M. A., Remmers, H., "Evaluation of vibration perception in passenger cabin", presented at DAGA 2004, Germany, 2004.

[4] Mansfield, N. J., Human Response to vibration, CRC Press, Boca Raton, ISBN 978-0415282390, 2005.

[5] Albertos, P., Sala, A., Multivariable control systems: an engineering approach, Springer, London, ISBN 978-1852337384, 2004.

[6] Vaes, D., Engelen, K., Anthonis, J., Swevers, J., Sas, P., "Multivariable feedback design to improve tracking performance on tractor vibration test rig", *Mech. Sys. and Sig. Proc.*, **21**(2):1051-1075, 2007.

[7] Strang, G. Linear algebra and its applications, Thomson Learning, Mason, ISBN 978-0155510050, 1986.

[8] Press, W. H.; Teukolsky, S. A.;Vetterling, W. T.;Flannery, B. P., Numerical Recipes in C: The art of scientific computing, Cambridge University, Cambridge, ISBN 978-0521431088, 2002.

[9] Bendat, J. S.; Piersol, A. G., Engineering applications of correlation and spectral analysis, John Wiley & Sons, New York, ISBN 0-471-57055-9, 1993.

[10] Silva, C. W. Vibration and shock handbook, CRC Press, Boca Raton, ISBN 978-0849315800, 2005.

CONTACT INFORMATION

Luiz CHAMON
Noise & Vibration Group – University of São Paulo
Mechanical Engineering Department
Av. Prof. Mello Moraes, 2231, sala TS08
05508-900 - São Paulo/SP - Brazil
Tel: +55 11 3091-9670
email: chamon@usp.br

ACKNOWLEDGMENTS

This research is part of the "Cabin Comfort" project at the University of São Paulo supported by the São Paulo Research Foundation (FAPESP).